Path-integral theory of the scattering of ^{4}He atoms at the surface of liquid ^{4}He

D. R. Swanson and D. O. Edwards
Physics Department, The Ohio State University, Columbus, Ohio 43210
(Received 31 July 1987)

The path-integral theory of the scattering of a ^{4}He atom near the free surface of liquid ^{4}He, which was originally formulated by Echenique and Pendry, has been recalculated with use of a physically realistic static potential and atom-ripplon interaction outside the liquid. The static potential and atom-ripplon interaction are based on the variational calculation of Edwards and Fatouros. An important assumption in the path-integral theory is the "impulse approximation": that the motion of the scattered atom is very fast compared with the motion of the surface due to ripplons. This is found to be true only for ripplons with wave vectors smaller than $q_m \sim 0.2$ Å^{-1}. If ripplons above q_m made an important contribution to the scattering of the atom there would be a substantial dependence of the elastic reflection coefficient on the angle of incidence of the atom. Since this is not observed experimentally, it is argued that ripplons above q_m give a negligible effect and should be excluded from the calculation. With this modification the theory gives a good fit to the experimental reflection coefficient as a function of the momentum and angle of incidence of the atom. The new version of the theory indicates that there is a substantial probability that an atom may reach the surface of the liquid without exciting any ripplons. The theory is not valid when the atom enters the liquid but analysis of the experiments shows that, once inside the liquid, the atom has a negligible chance of being scattered out again.

I. INTRODUCTION

Measurements of the scattering of atoms at the free surface of liquid helium are potentially a way to determine the properties of the surface. Such experiments have been carried out on the ^{4}He surface[1,2] using a beam of ^{4}He atoms and, to a limited extent,[3] a beam of ^{3}He. The results, in Fig. 1, show that the elastic scattering probability $R(\mathbf{k})$ for ^{4}He atoms striking the surface with momentum $\hbar\mathbf{k}$, depends only on the perpendicular[4] component of the wave vector $k_z = k\cos\theta$. The probability of inelastic scattering is found to be insignificantly small, so that the probability of absorption into the liquid is $1-R(k_z)$. We would like to find a theory which fits these measurements and, if possible, gives information about the ^{4}He surface: the density profile, correlation function, ripplon spectrum, or other properties.

The variational theory of Edwards and Fatouros[5] (the solid line in Fig. 1) gives a very good fit to the earlier measurements of $R(k_z)$, and it predicted the rise towards $R(k_z)=1$ which was observed below $k_z=0.03$ Å^{-1} in the later measurements[2] at glancing incidence. (These are shown in Fig. 1.) It also gives good results for the bound states[6,7] of ^{3}He on the surface of bulk ^{4}He and ^{4}He films,[7] and roughly agrees with the surface tension[8] of bulk ^{4}He. Nevertheless there is considerable doubt as to the validity of the approximations made in the theory, the accuracy of the density profile deduced from it (which is probably too narrow[9]) and the role of the ripplon and phonon excitations in the scattering.

The aim of the present paper is to investigate the role of the ripplons in the scattering. The elegant path integral theory of Echenique and Pendry[10] (EP) deals specifically with this point and it apparently shows that the creation of one or more ripplons is the principal mechanism for the absorption of most atoms into the liquid. However, the original calculation gave rather poor agreement with experiment, and it was not clear whether this was due to the central approximation in the theory, the restriction to a certain class of trajectories in the path integral, or to other simplifications.

We have modified the EP theory to improve the accuracy of some of the approximations but without changing the choice of trajectories. The modified form of the theory is much closer to experiment, although there is still some uncertainty in its predictions. The uncertainty is partly due to our poor knowledge of the effective Lagrangian of the system and in particular the effective interaction between the scattered atom and the ripplons or other modes of excitation of the liquid. Another, perhaps more important, difficulty is with the "impulse approximation." This assumes the motion of the atom to be fast compared with the motion of the surface due to ripplons. We find that this is not a valid approximation for a large proportion of the ripplon modes contributing to the scattering in the original form of the theory. The effect of these high-frequency modes is overestimated by the theory, and if they are omitted, the agreement with experiment is very satisfactory. This version of the theory shows that EP overestimated the number of ripplons produced by an atom, although it is still true that the majority of atoms excite one or more ripplons before reaching the liquid.

In the next section we review the theories currently in the literature to establish the context of the present work. Section III describes the EP theory in more detail, and discusses the approximations involved. It is pointed out that the impulse approximation implies that

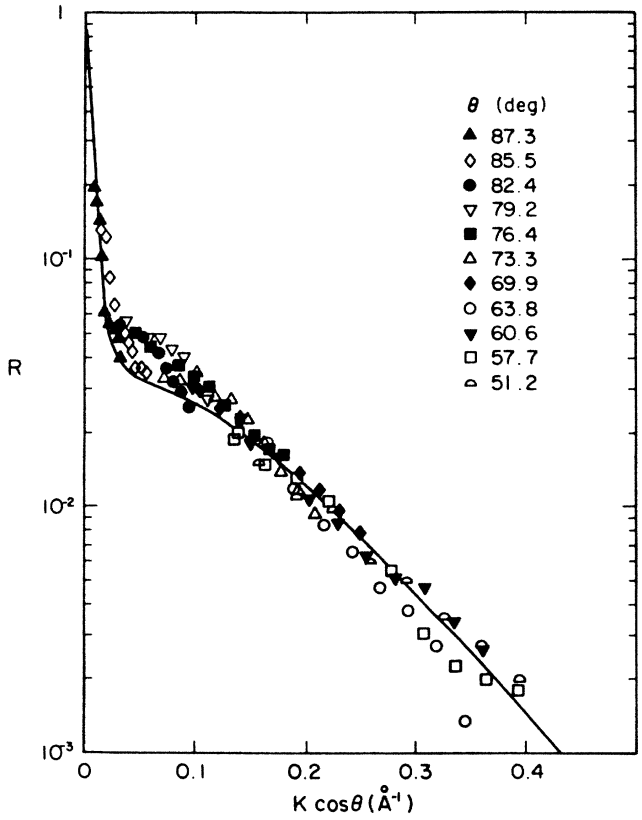

FIG. 1. The elastic scattering probability R as a function of the perpendicular wave vector $k_z = k\cos\theta$, for ^{4}He atoms incident on the liquid ^{4}He surface (from Ref. 2). The solid line is the EF theory (Ref. 5) which was fitted to earlier data (Ref. 1) from $k_z = -0.05$ to 0.6 Å^{-1} and angle of incidence θ from 13° to 70°. The asymptotic behavior $R \to 1$ as $k_z \to 0$, observed below $k_z \sim 0.03$ Å^{-1}, was predicted by the theory. In agreement with the theory, neither set of measurements shows any dependence on θ within the experimental scatter.

no transverse momentum is exchanged between the atom and the ripplons. Sections IV and V describe our modifications of the EP theory and the results, and Sec. VI gives some conclusions.

II. CURRENT THEORIES

There are four theories of atomic scattering at the surface of liquid ^{4}He in the literature.

(1) The theory of Edwards and Fatouros[5] (EF) is variational, with a trial function in the form suggested by Feynman[11] to represent a single impurity atom in liquid ^{4}He: $\Psi = f(\mathbf{r}_1)\Psi_0(\mathbf{r}_1, \ldots, \mathbf{r}_N)$, where Ψ_0 is the ground-state wave function for N ^{4}He atoms and $f(\mathbf{r}_1)$ is a function of $\mathbf{r}_1$, the position of the scattered "impurity" atom. Minimization of the energy gives a single-particle Schrödinger equation with an effective potential $V_{\rm eff}(z)$ which is related to the density $\rho(z)$ in the liquid ^{4}He ground state:

$$V_{\rm eff} = (\hbar^2/2m)a''/a - L_4 ,$$
$$a(z) \equiv \sqrt{\rho(z)/\rho_0} , \qquad (1)$$
$$a''(z) = d^2a/dz^2 .$$

In these equations, m is the mass of a ^{4}He atom, ρ_0 is the density in the interior of the liquid, and L_4 is the binding energy in the ground state, $L_4/k_B = 7.15$ K at zero pressure. EF constructed a formula for $a(z)$ which interpolates between the asymptotic behavior far above the liquid, where $V_{\rm eff} \to -\alpha/z^3$, and deep inside the liquid, where $V_{\rm eff} \to -L_4$:

$$a(z) = 1/\{1+\exp[p(z)]\} ,$$
$$p(z) = \beta z - g_1 + \lambda/[4\beta(z^2+g_2)] . \qquad (2)$$

Here $\beta = 1.087$ Å^{-1} is defined so that $L_4 = \hbar^2\beta^2/2m$. The van der Waals potential above the liquid is $-\alpha/z^3 = -\hbar^2\lambda/(2mz^3)$, where EF used the value $\lambda = 20$ Å. The constants $g_1 = 2.5$ and $g_2 = 8.5$ Å^2 were adjusted to give a fit to the first set of elastic scattering data.[1] The resulting effective potential is shown as the curve EF in Fig. 2.

Although the variational wave function Ψ is unsymmetrized with respect to the scattered atom at $\mathbf{r}_1$, an extremely good fit to experiment is obtained (Fig. 1). EF also tried a completely symmetrized Feynman wave function. In the liquid region of the coordinate space the symmetrized wave function represents a single phonon or roton formed by the absorption of the incident atom. The single-particle Schrödinger equation becomes an integro-differential equation. Even when elaborated to allow for the production of many phonons, this version of the theory predicts a large reflection probability for incident atoms with transverse momentum greater

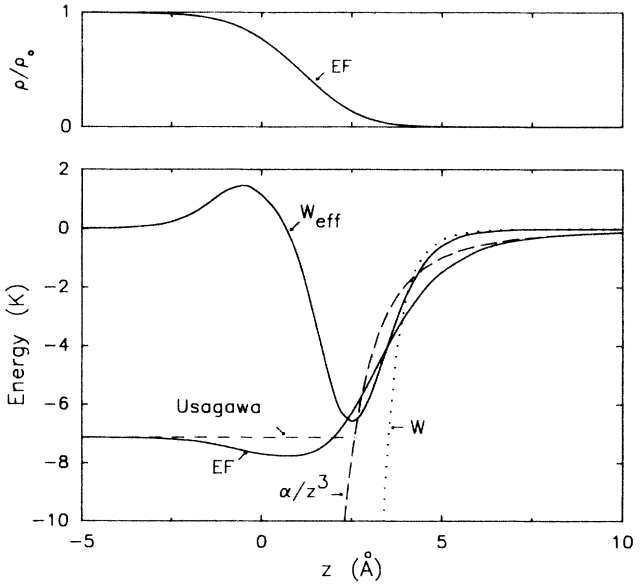

FIG. 2. (Top): The density profile ρ/ρ_0 in the Edwards-Fatouros theory. (Bottom): The real and imaginary potentials in various theories. The solid curve labeled EF is the effective potential in the Edwards-Fatouros theory. The dashed curve is the static potential $-\alpha/z^3$ used by Echenique and Pendry (EP). This was truncated by Usagawa at $-L_4$, the energy per atom in the liquid (the horizontal dashed line). The dotted curve labeled W is the imaginary part of the potential $iW(z)$ in the EP theory for an atom with $k_z = 0.2$ Å^{-1}, while $W_{\rm eff}$ is the corresponding quantity in the present work calculated for $k_z = 0.2$ Å^{-1} and $q_m = 3$ Å^{-1}.

than a critical value. Since this is not observed, EF concluded that the production of one or more ripplon excitations must be a dominant factor in capturing most atoms into the liquid.

In the Appendix, we show that EF's treatment of the situation where the incident atom has sufficient energy to generate rotons, as well as phonons, is incorrect. The Appendix shows that, if the atom is totally reflected below the threshold energy, as the threshold is reached the symmetrized theory predicts a dramatic reduction in the reflection coefficient. The data of Nayak *et al.*[2] in Fig. 1 span the region of total reflection at several angles both above and below the threshold, which is at $k=0.50$ Å^{-1}. The reflectivity is small and shows no sign of total reflection, or a break at the roton threshold. This demonstrates that the excitation of ripplons is a dominant effect in the scattering.

An observation made by EF concerns the insensitivity of the reflection coefficient to $V_{\rm eff}$ in the "liquid" region where $\rho/\rho_0=a^2(z)$ is not very small compared to unity. For the EF profile this region is approximately $z \lesssim 3.5$ Å. Adding to $V_{\rm eff}$ a large real or imaginary term proportional to $a^2(z)$ has no measurable effect on $R(k_z)$. This means that the surface region where rotons and phonons are produced, and where the width of the density profile is defined, is "screened" from observation in elastic scattering measurements. This explains the discrepancy between the width of the EF density profile and that calculated by rigorous microscopic methods.[9] Changes in $V_{\rm eff}$ proportional to the amplitude $a(z)$ *do* affect $R(k_z)$, showing that the boundary of the "screened" region is quite well defined.

(2) Usagawa[12] calculated the reflection coefficient using the Born approximation assuming that the production of only one ripplon is important. This is in contrast to the EP theory which indicates that multiple ripplon production dominates. The Usagawa theory reduces to a one-dimensional Schrödinger equation which includes a nonlocal or velocity-dependent potential in addition to the static van der Waals potential V_s. The results (Fig. 3) show a dip near $k_z=0.07$ Å^{-1} not seen in the experiment. Usagawa attributed the dip to his use of a cutoff in the static potential near the surface where $V_s=-\alpha/z^3$ is joined to the binding energy $-L_4$ (see Fig. 2). For k_z above the dip the theoretical reflectivity is larger than experiment.

(3) In a recent paper Goodman and Garcia[13] (GG) show empirically that the effective potential, introduced by EF, can be replaced by a different formula without spoiling the agreement with experiment. The formula consists of $U(z)$, the expectation value of the potential energy for one atom in the ground state, truncated near the surface to $-L_4$, as in the Usagawa potential. GG thus show that the dip in Usagawa's reflection coefficient was *not* caused by the truncation in his potential.

To calculate $U(z)$, GG assume a simple step-function form for the two-body correlation function in the ground state. A more realistic correlation function might change the results significantly. A comparison between $V_{\rm eff}(z)$ and a realistic $U(z)$ for a hydrogen atom near the ^{4}He surface was made by Mantz and Edwards.[6] In that case the two potentials agreed only for $z \gtrsim 8$ Å.

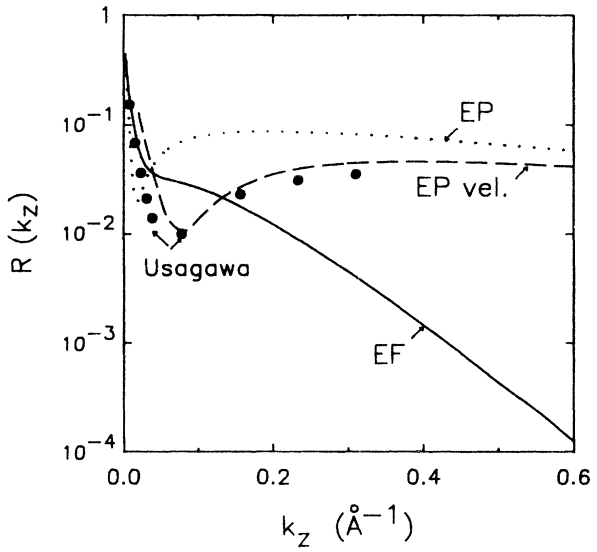

FIG. 3. The reflection coefficient R as a function of k_z in the EF theory (solid curve), and in the theory of Usagawa (the circles). The original Echenique-Pendry theory is labeled EP, while "EP-vel" corresponds to the trajectories given by Eq. (19). The experimental data agree with the EF curve.

(4) Echenique and Pendry:[10] EP show that multiple ripplon production occurs when an incident atom approaches to within a few angstroms of the surface. The effect of the ripplons in the Feynman path integral is eventually reduced to an imaginary and therefore absorptive part $iW(z)$ of the potential which adds to the static van der Waals potential V_s in a one-particle Schrödinger equation. The reflection coefficient calculated from the EP theory, shown in Fig. 2, is much larger than experiment. (Note that this curve is not the same as the one published by EP. The published curve was calculated using an intuitive truncation[14] of both $iW(z)$ and V_s at small z, which was not described in their paper.)

III. ECHENIQUE-PENDRY THEORY

We now describe the formalism of the EP theory, with some comments on the approximations. The Lagrangian includes the incident atom at position $\mathbf{r}$, the ripplons with horizontal wave vectors $\mathbf{q}$ and normal coordinates $A_{\mathbf{q}}$, and the interaction $\phi_{\mathbf{q}}A_{\mathbf{q}}$ between the ripplons and the atom due to the van der Waals interaction:

$$L=\sum_{\mathbf{q}}\left[\frac{1}{4}\frac{\rho_0}{q}(\dot{A}_{\mathbf{q}}^2-\omega^2A_{\mathbf{q}}^2)-\phi_{\mathbf{q}}(\mathbf{r})A_{\mathbf{q}}\right]$$
$$+\tfrac{1}{2}m\,|\dot{\mathbf{r}}|^2-V_s(z)\,. \tag{3}$$

The ripplon frequency ω is given by the dispersion relation $\omega^2=(\sigma/\rho_0)q^3$, σ is the surface tension[15] (0.354 erg/cm^2), ρ_0 is the bulk liquid mass density ($\rho_0=0.145$ g cm^{-3}), and $V_s(z)$ is the static van der Waals potential

acting on the atom. In the first version of their theory, where the density profile $\rho(z)$ at the surface is assumed to be a step function at $z=0$, EP take $V_s(z)$ to be

$$V_s=-\frac{\alpha}{z^3}=-\frac{\hbar^2\lambda}{2mz^3}\ , \tag{4}$$

with $\lambda=20.25$ Å, slightly larger than the EF value. In a second calculation the density profile was assumed to be linear in z over a width of 5 Å, but the ripplon spectrum and interaction were left unchanged. We consider only the first version of the theory.

In the path integral method the state of the system $\psi(X_2(t_2))$ at time t_2 can be derived from a previous state $\psi(X_1(t_1))$:

$$\psi(X_2)=\int F(X_2,X_1)\psi(X_1)dX_1\ , \tag{5}$$

where the X represent the generalized coordinates (in this case $\mathbf{r}$ and A_q), and $F(X_2,X_1)$ is the Feynman propagator, or path integral:

$$F(X_2,X_1)=\int_{X_1}^{X_2} e^{iS/\hbar}DX(t)\ . \tag{6}$$

This is the sum over all possible paths, from $X_1(t_1)$ to $X_2(t_2)$, of the probability amplitude $\exp(iS/\hbar)$ with the action S for each path given by

$$S=\int_{t_1}^{t_2} L(\dot{X},X,t)dt\ . \tag{7}$$

The assumption that the motion of the atom is very fast compared to the ripplon motion (the impulse approximation) simplifies Eq. (6). In this case the propagator depends only on the initial and final positions of the scattered atom:

$$\psi^+(\mathbf{r}_2)=\int \tilde{F}(\mathbf{r}_2,\mathbf{r}_1)\psi^-(\mathbf{r}_1)d\mathbf{r}_1\ . \tag{8}$$

Here $\psi^-(\mathbf{r}_1)$ is the incident wave packet and $\tilde{F}(\mathbf{r}_2,\mathbf{r}_1)$ is the Feynman propagator for an isolated atom moving in the potential $V_s(z)$ but modified by a factor γ:

$$\tilde{F}(\mathbf{r}_2,\mathbf{r}_1)=\int_{\mathbf{r}_1}^{\mathbf{r}_2} e^{i\tilde{S}/\hbar}\gamma\, D\mathbf{r}(t)\ , \tag{9}$$

$$\tilde{S}=\int_{t_1}^{t_2}[m\dot{\mathbf{r}}^2/2-V_s(z)]dt\ . \tag{10}$$

The factor γ, which is a functional of the trajectory of the atom, is the probability amplitude for *not* exciting any ripplons:

$$\gamma=\exp\left[-\frac{\Omega}{2\pi}\int_0^\infty \frac{\bar{\phi}_q^2}{2\hbar\rho_0\omega}q^2dq\right]\ , \tag{11}$$

where Ω is the area of the surface and $-\bar{\phi}_q$ is the classical impulse given to the ripplon mode $\mathbf{q}$ as the atom traverses the trajectory:

$$\bar{\phi}_q=\int_{-\infty}^{\infty}\phi_q(\mathbf{r}(t))dt\ . \tag{12}$$

The ripplon-atom interaction ϕ_q is found, to first order in the ripplon amplitude A_q, by integrating the $1/r^6$ van der Waals interatomic potential between the incident atom and the atoms in the liquid:

$$\phi_q=-\frac{3}{2\sqrt{\Omega}}\frac{\hbar^2\lambda}{2m}\cos(\mathbf{q}\cdot\mathbf{r}_\parallel)\frac{q^2}{z^2}K_2(qz)\ , \tag{13}$$

with K_2 the modified Bessel function of the second kind.

The central assumption in the EP theory is that the summation over paths can be approximated by a sum over the "classical" trajectories shown in Fig. 4. The atom follows a path with constant velocity except that $\dot{z}$ is reversed at some height z_0 which characterizes the trajectory:

$$z(t)=\frac{\hbar k_z}{m}\,|\,t\,|+z_0\ . \tag{14}$$

The integral over time in (12) is found by substituting from (14) and integrating over z. The $\cos(\mathbf{q}\cdot\mathbf{r}_\parallel)$ term in (13) is set equal to one. This precludes any angular dependence in the reflection coefficient. We have verified numerically that this approximation is valid up to $\approx 70°$. With these simplifications γ is found to be

$$\gamma(z_0)=\exp\left[-\frac{2\lambda^2m^2\epsilon}{\pi\hbar^3\sqrt{\rho_0\sigma}k_z^2z_0^{15/2}}\right]$$
$$=\exp\left[-\frac{1363\ \text{Å}^{11/2}}{k_z^2z_0^{15/2}}\right]\ , \tag{15}$$

where ϵ is the numerical constant:

$$\epsilon=\int_0^\infty dx\,x^{13/2}\left[\int_x^\infty dy\frac{K_2(y)}{y^2}\right]^2=0.390\ .$$

We have calculated ϵ to a higher accuracy than EP who used a value of 0.308. Equation (9) now becomes

$$\tilde{F}(\mathbf{r}_2,\mathbf{r}_1)=\int_{\mathbf{r}_1}^{\mathbf{r}_2} e^{iS'/\hbar}D\mathbf{r}(t)\ , \tag{16}$$

where

$$S'=\int_{t_1}^{t_2}\left[\tfrac{1}{2}m\dot{\mathbf{r}}^2-V_s(z)+i\hbar\,|\,\dot{z}\,|\,\frac{d\ln\gamma(z)}{2dz}\right]dt\ . \tag{17}$$

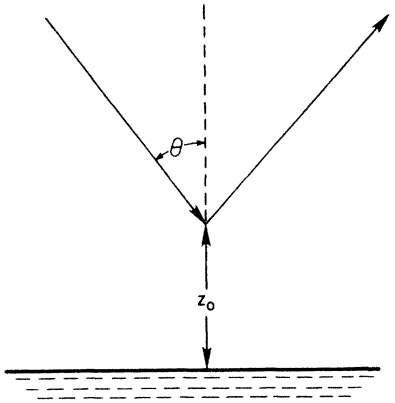

FIG. 4. The trajectory of an atom in the Echenique and Pendry theory. The horizontal and vertical components of the velocity are constant except at $z=z_0$ where $\dot{z}$ is reversed.

Thus the effect of ripplon production is the same as that from an imaginary term in the potential,

$$iW(z,k_z)=i(\hbar\,|\,\dot{z}\,|\,/2)d\,\ln\gamma\,/dz\ , \tag{18}$$

proportional to $1/(k_z z^{17/2})$. The elastic reflection coefficient $R(k_z)$ is found by numerical integration of the one-dimensional Schrödinger equation with potential $V_s(z)+iW(z,k_z)$. The solution is started at small, positive z where the absorptive part of the potential is very strong. Provided z is small enough it does not matter where the solution is started.

The resulting reflection coefficient is labeled EP in Fig. 3, which also shows the effect of using a slightly different "classical" trajectory which conserves energy as well as transverse momentum:

$$|\,\dot{z}\,|=[\hbar^2k_z^2-2mV_s(z)]^{1/2}/m\ . \tag{19}$$

These variable velocity trajectories give a result which is only a small improvement over the original theory.

A. Impulse approximation and conservation of transverse momentum

An important approximation in the EP theory, which greatly simplifies the calculation, is the assumption that the trajectory of the atom is traversed very rapidly compared with the motion of the ripplons: the impulse approximation. The characteristic time for an atom traversing the lower part of the trajectory in Fig. 4 is $\tau_0\approx mz_0/\hbar k_z$. For a ripplon mode of angular frequency ω, the impulse approximation requires $\omega\tau_0\ll 1$ or, in terms of q,

$$q<q_c=(\rho_0\hbar^2k_z^2/m^2z_0^2\sigma)^{1/3}\ . \tag{20}$$

Taking $z_0\sim 5$ Å, $k_z\sim 0.5$ Å^{-1}, we find $q\lesssim 0.2$ Å^{-1} for the impulse approximation to be valid.

The impulse approximation has important physical consequences. The ripplon modes assumed by EP correspond to the standing waves $A_{\mathbf{q}}(t)\cos(\mathbf{q}\cdot\mathbf{x})$ and $B_{\mathbf{q}}(t)\sin(\mathbf{q}\cdot\mathbf{x})$, where $\mathbf{x}$ represents the horizontal position on the surface. If $\mathbf{x}=0$ at the lowest point of the trajectory of the atom (Fig. 4), the coupling of the atom to the sine modes, with normal coordinates $B_{\mathbf{q}}$, is zero in the impulse approximation. The atom does not couple to the standing-wave state $|\,\mathbf{q}\rangle-|\,-\mathbf{q}\rangle$, only to $|\,\mathbf{q}\rangle+|\,-\mathbf{q}\rangle$, where $|\,\mathbf{q}\rangle$ is the ripplon travelling-wave state with momentum $\hbar\mathbf{q}$. This shows that EP chose the appropriate set of standing-wave states and that there is no exchange of transverse momentum to the ripplons in the impulse approximation. The atoms which lose energy to the ripplons enter the liquid with their transverse momentum intact.

When the impulse approximation breaks down, the atom may transfer some of its horizontal momentum to the ripplons. For instance, a ripplon wave-packet traveling with a velocity which matches the horizontal motion of the atom is more strongly coupled than others which are mismatched. Therefore ripplon modes for which the impulse approximation is invalid should produce a dependence of the reflectivity $R(k_z)$ on θ as well as k_z. The experimental data show little or no θ dependence indicating that ripplons with $q\gtrsim q_c\approx 0.2$ Å^{-1} have little or no effect on the scattering.

The prediction that there is no horizontal momentum given to the ripplons is consistent with the experiment of Edwards, Ihas, and Tam[16] who observed the angular and time-of-flight distribution of the phonons and rotons produced in the liquid by a beam of ^{4}He atoms. The results indicated that the atoms, on average, lose energy to the ripplons but conserve their transverse momentum.

IV. MODIFIED ECHENIQUE-PENDRY THEORY

The disagreement between the EP theory and experiment could be due to the oversimplified static potential V_s and ripplon-atom interaction $\phi_{\mathbf{q}}$, both of which have singularities at the liquid surface $z=0$. These singularities remain when the density profile is not assumed to be a step function. EP argued that the singularities do not matter because the beam is reflected or absorbed a few angstroms above the liquid, so that the results are independent of V_s and W very close to the surface. Our numerical calculations show that this is not true and, in any event, EP found it necessary to truncate V_s and W to obtain a result closer to experiment.

The singularities in V_s and $\phi_{\mathbf{q}}$ are due to neglect of the correlations between the incident atom and those in the liquid. The correlations are, at least approximately, taken into account in the variational wave function used by EF. Therefore, in our version of the path integral theory, we replace the static potential V_s by the EF effective potential $V_{\rm eff}$. This also takes into account the approximate width and shape of the density profile $\rho(z)$ at the surface.

The variational theory could also be used to find a more accurate formula for $\phi_{\mathbf{q}}$, the interaction between the scattered atom and a ripplon of wave vector $\mathbf{q}$. One would use a trial wave function which represents the scattered atom and the liquid with one ripplon excited. Rather than attempting this, we have constructed an approximation for $\phi_{\mathbf{q}}$ which is correct at all z for $q=0$, and for $q>0$, has the correct asymptotic properties as $z\to\infty$. This approximation replaces $3\alpha K_2(qz)/z^2$ in Eq. (13) by $(z-z_s)^2V'_{\rm eff}K_2(q\,|\,z-z_s\,|\,)$:

$$\phi_{\mathbf{q}}^{\rm eff}=-\frac{\cos(\mathbf{q}\cdot\mathbf{r}_{\parallel})}{2\sqrt{\Omega}}\frac{dV_{\rm eff}}{dz}(qs)^2K_2(qs)\ , \tag{21}$$

where $s\equiv|\,z-z_s\,|$. The quantity $z_s=1/(2\beta)=0.46$ Å appears in these formulas because the effective EF potential $V_{\rm eff}\to-\alpha/(z-z_s)^3$ for large z. This means that, as seen by the atom, the effective position of the surface is at $z=z_s$ rather than $z=0$.

A ripplon mode with $q=0$ corresponds to a translation of the surface up or down so that $\phi_{q=0}$, to first order, is given by

$$\phi_{q=0}=(1/\sqrt{\Omega})dV_{\rm eff}/dz\ .$$

Equation (21) agrees with this since $(qs)^2K_s(qs)=2$ at $q=0$.

Equation (21) also has the correct asymptotic form for

large z where $V'_{\rm eff}\to 3\alpha/(z-z_s)^4$. In this limit, $\phi_q^{\rm eff}$ reduces to the same form as that calculated by EP, but with the surface at z_s.

In contrast with the original formula (13), Eq. (21) is well behaved at all values of z. Although we have no way to determine the real particle-ripplon interaction when $z-z_s$ is close to zero or negative, (21) gives a $\phi_q^{\rm eff}$ which is smooth at the surface and goes to zero inside the liquid.

For simplicity we have retained the ripplon spectrum $\omega^2=(\sigma/\rho_0)q^3$ although deviations from this simple formula become substantial[17] for wavelengths approaching the thickness of the surface. Although it would have been easy to carry out the numerical calculations with a different $\omega(q)$, consistency would require the inclusion of the coupling to the phonon and roton modes as well. The simple formula $\omega^2=(\sigma/\rho_0)q^3$ is appropriate to a liquid with a sharp surface and which is incompressible, so that it has no phonon modes.

With the simple ripplon spectrum there is an infinity in the integral over q in Eq. (11) at $q\to\infty$ and $z=z_s$. This can be suppressed by taking an upper limit q_m for this integral, so that the effects of ripplon modes with $q>q_m$ are not included in the scattering amplitude. We find that $q_m\sim 3$ Å^{-1} eliminates the effects of the infinity while at the same time the results are independent of q_m. Ripplons with $q\gtrsim 3$ Å^{-1} correspond to energies greater than ~ 60 K according to the ripplon spectrum we are using. The energy available to excite a ripplon is only $L_4+\hbar^2k_z^2/2m$: no more than ~ 10 K. Therefore the value of q_m does not matter provided it is sufficiently large.

The cutoff q_m may also be used in another, more physical way: to eliminate ripplons with wavelengths smaller than the thickness of the surface. The ripplon spectrum[17] $\omega(q)$ and the interaction ϕ_q are largely unknown in this range. In addition the impulse approximation is invalid for ripplons with q larger than q_c. In the EP theory q_c, given by (20), depends on the trajectory and on k_z but is approximately 0.2 Å^{-1}, corresponding to ripplons of energy ~ 1 K. By choosing $q_m\sim q_c$ we can study the contribution to $R(k_z)$ from ripplons outside the impulse approximation. As we shall see, the numerical results show that including these ripplons gives large deviations from experiment and, in particular, a substantial dependence of $R(k_z)$ on θ. The absence of any θ dependence in the experimental data seems to indicate that the effect of ripplons with $q>q_c$, if it could be properly calculated, is actually quite small.

One should note that, of course, decreasing q_m always shifts the results closer to experiment since, in the limit of $q_m\to 0$, the effect of the ripplons disappears and the theory reduces to that of EF. The EF potential was adjusted to fit the data without the ripplons, so that it may not be the correct effective potential. We have not tried to readjust $V_{\rm eff}$.

With these modifications the impulse transferred to the atom $\bar\phi_{\rm q}^{\rm eff}$ becomes

$$\bar\phi_{\rm q}^{\rm eff}=\int_{-\infty}^{\infty}\phi_q^{\rm eff}(\mathbf{r}(t))dt$$

$$=-2\int_{z_0}^{\infty}\frac{1}{2\sqrt{\Omega}}\cos(\mathbf{q}\cdot\mathbf{r}_\parallel)\frac{dV_{\rm eff}(z)}{dz}$$

$$\times(qs)^2K_2(qs)\frac{dz}{|\dot z|}\ . \tag{22}$$

The velocity $|\dot z|$ is given by the analog of Eq. (19) with V_s replaced with $V_{\rm eff}$. To keep the angular dependence, the term $\mathbf{q}\cdot\mathbf{r}_\parallel$ must be calculated as a function of z:

$$\mathbf{q}\cdot\mathbf{r}_\parallel(z)=\mathbf{q}\cdot\dot{\mathbf{r}}_\parallel(z)t(z,z_0,k_z)$$

$$=q\frac{\hbar k_z}{m}\tan\theta\, t(z,z_0,k_z)\cos\xi\ , \tag{23}$$

with

$$t(z,z_0,k_z)=\int_{z_0}^{z}\frac{dz'/m}{[\hbar^2k_z^2-2mV_{\rm eff}(z')]^{1/2}}\ ,$$

where ξ is the angle between $\mathbf{q}$ and $\mathbf{r}_\parallel$.

The effective attenuation factor $\gamma_{\rm eff}$, which replaces γ, is given by

$$\gamma_{\rm eff}=\exp\left[-\frac{\Omega}{(2\pi)^2}\int_{-\pi}^{\pi}d\xi\int_0^{q_m}dq\,q^2\frac{(\bar\phi_{\rm q}^{\rm eff})^2}{2\hbar\rho_0\omega}\right]\ . \tag{24}$$

The derivative of $\ln(\gamma_{\rm eff})$ with respect to z_0 contributes two terms to $W_{\rm eff}$ [see (18)]. One term comes from the integral over z in (22). The second comes from the dependence of $\mathbf{q}\cdot\mathbf{r}_\parallel$ on z_0 in (23). The second term is zero for $\theta=0$ and we have verified numerically that it is negligible for $\theta>0$. Thus the effective imaginary potential is

$$iW_{\rm eff}(z_0,k_z,\theta)=-\frac{i}{4\pi\sqrt{\rho_0\alpha}}\frac{dV_{\rm eff}(z_0)}{dz_0}\int_0^{q_m}dq\,\sqrt{q}\,(qs_0)^2K_2(qs_0)$$

$$\times\int_{z_0}^{\infty}dz(qs)^2K_2(qs)\frac{dV_{\rm eff}(z)}{dz}\frac{J_0[q(\hbar k_z/m)\tan\theta\, t(z,z_0,k_z)]}{[\hbar^2k_z^2-2mV_{\rm eff}(z)]^{1/2}/m}\ , \tag{25}$$

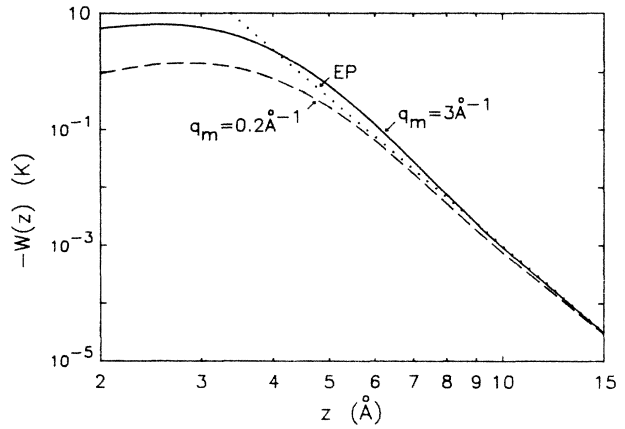

FIG. 5. The imaginary part of the potential in the Echenique and Pendry (EP) theory and the same quantity in the present work for two values of the ripplon cutoff q_m.

with

$$s_0 = |z_0 - z_s| \ .$$

V. RESULTS

The result of evaluating Eq. (25) numerically is shown in Figs. 2 and 5 for $k_z = 0.2$ Å^{-1} and $q_m = 3$ Å^{-1}. Note that $iW_{\text{eff}}(z)$ is positive for some values of z. A positive imaginary potential indicates the "creation" of particles in the beam. This corresponds to a multiple interaction between an atom and a ripplon mode. The atom loses some energy interacting with the ripplon field and is knocked out of the beam. The atom interacts again with the ripplon field regaining its energy and resuming its place in the beam. This process also explains why ripplon modes of energy $\hbar\omega$ larger than the energy available from the atom $L_4 + \hbar^2 k_z^2/2m$ can, in principle, influence the reflection coefficient. However, the behavior of W_{eff} below $z = 3.5$ Å is mostly academic since EF showed that $R(k_z)$ is not sensitive to this region.

An important conclusion from the EP theory is that atoms approaching within approximately 5 Å of the surface always produce one or more ripplons. A plot of $1 - |\gamma_0|^2 \equiv 1 - |\gamma|^2$, the probability of completing a trajectory with the creation of at least one ripplon, is shown in Fig. 6. Also shown is a plot of $|\gamma_1|^2$, the probability of creating one and only one ripplon. The probability of exciting n ripplons $|\gamma_n|^2$ is related to $|\gamma_0|^2$ by

$$|\gamma_n|^2 = |\gamma_0|^2 [-\ln |\gamma_0|^2]^n / n! \ . \tag{26}$$

The probability of exciting no ripplons $|\gamma_0|^2$ may be calculated using Eq. (24), or by integrating Eq. (18):

$$\gamma_0 = \exp\left[-2 \int_{z_0}^{\infty} \frac{W_{\text{eff}}(z)}{\hbar |\dot{z}|} dz \right] \ . \tag{27}$$

Our results, the full curves in Fig. 6, are calculated for $q_m = 3$ Å^{-1}. Note that $1 - |\gamma_0|^2 - |\gamma_1|^2$ is the probability for creating more than one ripplon. As in the original EP theory, we find that this is appreciable below $z \sim 5$ Å.

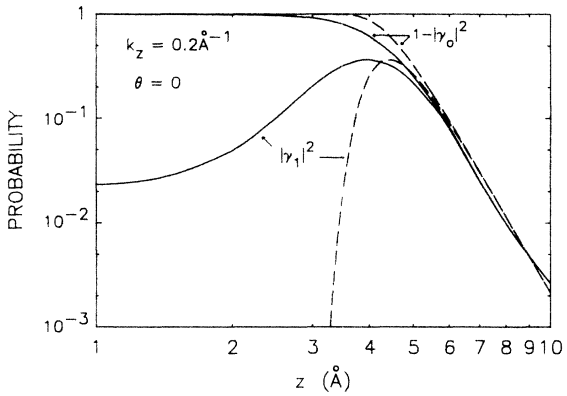

FIG. 6. The probability $|\gamma_1(z)|^2$ of completing a trajectory with the creation of only one ripplon, and the probability $1 - |\gamma_0|^2$ of creating one or more ripplons, for an atom with $k_z = 0.2$ Å^{-1} at normal incidence ($\theta = 0$). The solid curves are the present theory calculated with the ripplons above $q_m = 3$ Å^{-1} omitted. The dashed curves are the EP theory calculated with the variable velocity trajectories of Eq. (19).

Figure 7 shows the dependence of $1 - |\gamma_0|^2$ on q_m, the cutoff in the ripplon spectrum, at two different values of k_z and at normal incidence, $\theta = 0$. The cutoff has a strong effect, particularly at large values of k_z. The probability that an atom with $k_z = 0.6$ Å^{-1} excites at least one ripplon is substantially reduced for $q_m = 0.2$ Å^{-1}. This value of q_m is the most plausible one since it excludes ripplons whose frequency is too high for the impulse approximation to be valid. The absence of any measurable θ dependence in the experimental data indicates that these ripplons do not contribute to the reflection coefficient. Moreover it is clear that, if the motion of the high-frequency ripplon modes were taken

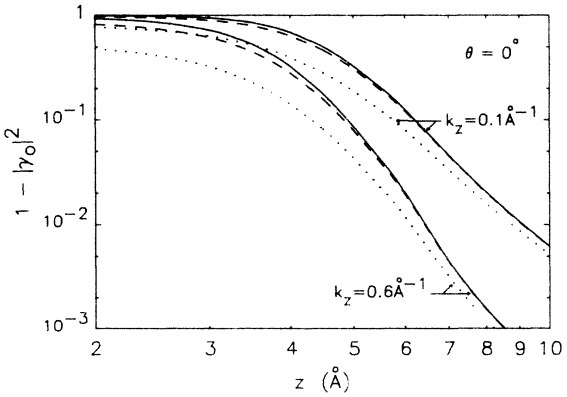

FIG. 7. The probability $1 - |\gamma_0|^2$ of completing a trajectory with the creation of one or more ripplons, for an atom with $k_z = 0.1$ or 0.6 Å^{-1}, for various values of the ripplon cutoff q_m. The dotted curves are calculated for $q_m = 0.2$ Å^{-1}, the dashed curves for $q_m = 0.5$ Å^{-1}, and the solid curves are for $q_m = 3$ Å^{-1}.

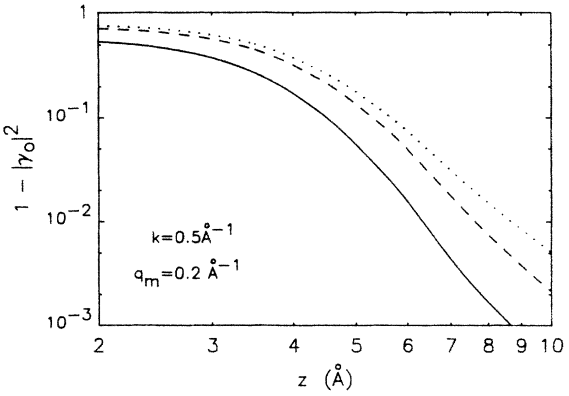

FIG. 8. The effect of the angle of incidence on the probability $1-|\gamma_0|^2$ of completing a trajectory with the creation of one or more ripplons, at constant total wave vector $k=0.5$ Å^{-1}. The solid curve is for $\theta=0$ (normal incidence), the dashed curve is for $\theta=70°$ ($k_z=0.17$ Å^{-1}), and the dotted curve is for $\theta=87°$ ($k_z=0.026$ Å^{-1}).

into account, the impulse transferred to them by the atom would be reduced below that given by Eqs. (12) and (22).

The effect of the angle of incidence on $1-|\gamma_0|^2$ is shown in Fig. 8. For $q_m=0.2$ Å^{-1}, the figure shows that $1-|\gamma_0|^2$ increases considerably with θ, at constant total wave vector k. At constant k_z, it decreases with θ but, as we shall see, the predicted reflection coefficient hardly depends on θ.

The reflection coefficient, $R(k_z,\theta)$ is found by numerical integration of the one-dimensional Schrödinger equation:

$$-\frac{\hbar^2}{2m}\frac{d^2\psi}{dz^2}+[V_{\text{eff}}(z)+iW_{\text{eff}}(z,k_z,\theta)]\psi=\frac{\hbar^2k_z^2}{2m}\psi\ . \quad (28)$$

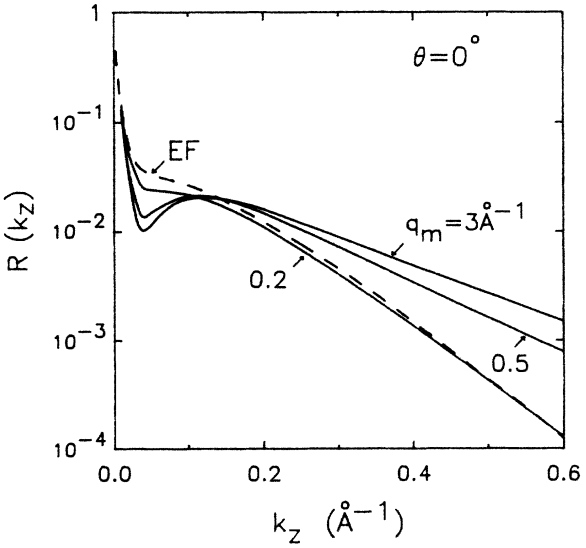

FIG. 9. The reflection coefficient $R(k_z)$ calculated with various ripplon cutoffs, $q_m=0.2$, 0.5, or 3 Å^{-1}. Ripplons with wave vectors above 0.2 Å^{-1} are outside the range of the impulse approximation. The Edwards-Fatouros (EF) curve, which is a good fit to the data, is shown for comparison.

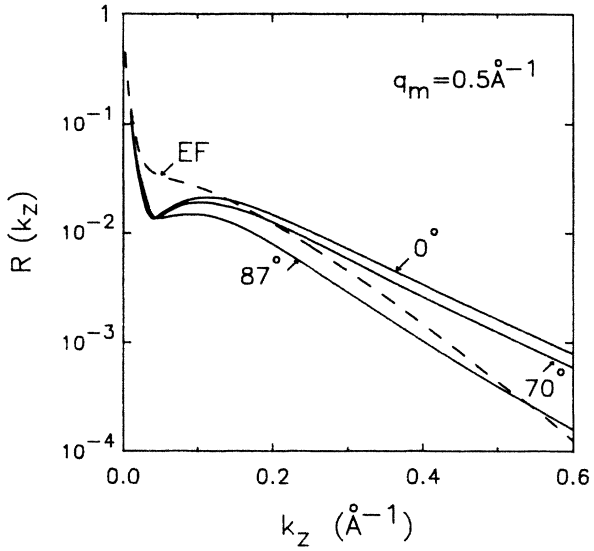

FIG. 10. The reflection coefficient $R(k_z,\theta)$ calculated for angles of incidence up to 87° with $q_m=0.5$ Å^{-1}. These curves show an angular dependence not seen in the experimental data.

The solution is started deep inside the liquid where $V_{\text{eff}}\to -L_4$ and $iW_{\text{eff}}\to 0$.

The reflection coefficient calculated for three values of the cutoff q_m is shown in Figs. 9, 10, and 11 as a function of k_z and θ. Only for $q_m=0.2$ Å^{-1} are the results in satisfactory agreement with experiment, with negligible angular dependence, and in close agreement with the EF theory.

The effect of our more realistic V_s and ϕ_q, and the cutoff $q_m\approx 0.2$ Å^{-1}, is to reduce the ripplon creation compared to the EP theory. According to Figs. 7 and 8 there is a substantial probability that an atom can

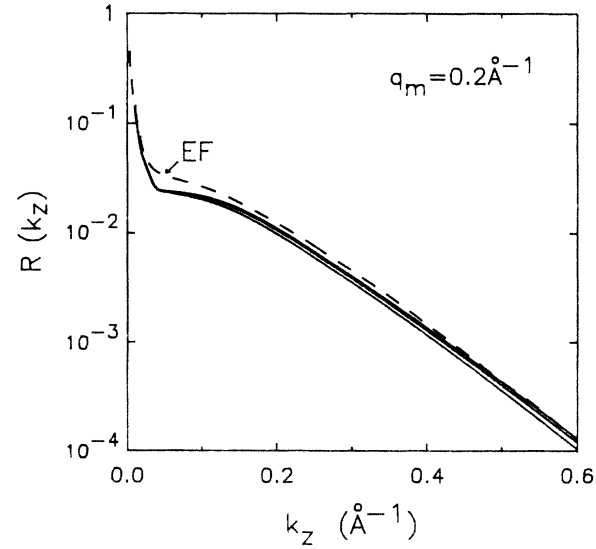

FIG. 11. The reflection coefficient $R(k_z)$ calculated for 0°, 70°, and 87° angles of incidence with $q_m=0.2$ Å^{-1}, the approximate upper limit in the impulse approximation. The 0° curve is the highest of the three and the 87° curve the lowest. There is very little angular dependence in good agreement with experiment.

penetrate the surface without producing a single ripplon. It would then be able to produce a roton or single or multiple phonons, provided transverse momentum and energy can be conserved. However, in the region of the surface, the indistinguishability of the scattered atom from those in the liquid becomes a dominant factor, which the path integral theory does not take into account. Moreover we cannot calculate $|\gamma_0|^2$ or $V_{\rm eff}$ when the atom enters the liquid.

VI. DISCUSSION AND CONCLUSION

A fairly clear and consistent picture of scattering at the helium surface can be drawn from the path integral theory, from the variational results of EF and from the experimental data. Although this picture is not substantially different from that drawn by EF (see their "Discussion" section), some additional details have been added. We describe this picture here.

The space where scattering takes place can be divided into two regions: the "screened region" below $z \approx 3.5$ Å on the scale defined by the EF effective potential, and the "unscreened" region where $z > 3.5$ Å. The properties of the two regions are as follows.

A. Unscreened region ($z > 3.5$ Å)

According to EF, substantial changes in the real or imaginary potential in the screened region have no appreciable effect on the reflectivity $R(kz)$. Therefore all the elastic reflection of atoms takes place in the unscreened region.

According to the path-integral theory, excitation of ripplons below the cutoff for the impulse approximation, $q_m \sim 0.2$ Å^{-1}, takes place in the unscreened region. The fact that ripplons above this cutoff, which corresponds to a ripplon energy of ~ 1 K, do not contribute much to the scattering in the unscreened region is deduced from the lack of any θ dependence in $R(k_z)$. Since the ripplon modes which *are* excited can be treated within the impulse approximation, the transverse momentum of the atom is conserved in the unscreened region. In addition, Fig. 11 shows that the excitation of ripplons with $q < 0.2$ Å^{-1} has little or no effect on the reflection coefficient.

Although no explicit calculations have been carried out, it seems plausible that the excitation of ripplons in this region produces negligible inelastic scattering, in agreement with the experiments.

The results in Sec. V show that, although the majority of incident atoms excite ripplons in the unscreened region, there is a substantial probability for atoms to reach the liquid without exciting a ripplon. This accounts for the observation by Baird *et al.*[18,19] of single phonon or roton events: the evaporation of an atom by a phonon or roton apparently with conservation of energy and transverse momentum. This is the inverse of the process in which an atom passes unscathed through the unscreened region to create a single phonon or roton in the liquid.

Note that, in the present picture, there is no contradiction between the observation of single-roton events[19,20] and the absence of any measurable feature in the reflection coefficient or in the spectrum of evaporated atoms[21] at the roton threshold. The creation of the roton by the atom takes place in the screened region, and consequently it does not affect the reflection coefficient.

B. Screened region ($z < 3.5$ Å)

In the screened region of space, where the density of the liquid is substantial, the effect of symmetry is important: The symmetric EF theory differs from the unsymmetrized version when the amplitude function $a(z) = \sqrt{(\rho/\rho_0)}$ is not negligible compared to unity. In the surface part of this region, where the width of the density profile is defined, even the static effective potential $V_{\rm eff}$ is unknown. However, it is clear that the screened region is highly absorptive, or "black" as far as scattered atoms are concerned. More precisely, the probability amplitude, as defined in the context of the path-integral theory, for an atom reaching this region and to be reflected out is extremely low. This is inferred from the atomic scattering data at glancing incidence. No vestige of total reflection from the single-phonon or multi-phonon channels is seen in these data either above or below the roton threshold. We deduce that, below the roton threshold, any atom which does not produce a phonon or phonons, produces *ripplons* in the screened region.

If no ripplons have been produced in the unscreened region, an atom which has reached the screened region has a high energy, at least $L_4 = (7.15\ \text{K})k_B$. Consequently the ripplons produced in the screened region may include both high and low frequencies. There is no satisfactory microscopic theory for the production of high-energy ripplons (or even for their energy spectrum) or for the production of protons or phonons in the surface part of the screened region.

The picture we have drawn and the predictions of the path-integral theory could be tested quantitatively by measurements of the probability of the various absorption and excitation processes in the liquid. For instance, it would be useful to know the fraction of the atoms with incident momentum $\hbar\mathbf{k}$ which convert directly into single excitations in the liquid. This fraction should be no larger than the probability predicted by the path-integral theory for such atoms to reach the liquid without producing low energy ripplons (< 1 K) on the way. Alternatively the probability for a single-energetic excitation to produce a single atom might be measured. This is related by detailed balance to the probability of the inverse process.

ACKNOWLEDGMENTS

This work was supported by National Science Foundation (Low Temperature Physics Program) Grants No. DMR-79-01073 and No. DMR-84-03441. We are grateful to Professor R. L. Mills for valuable discussions about the Appendix.

APPENDIX

In this appendix we treat the problem of calculating the reflection coefficient in the symmetrized EF theory

when the energy of the incident atom is above the threshold for the creation of a roton. In this situation there are three solutions to the single-particle Schrödinger-type integro-differential equation [(21) in EF] which have the same energy $\hbar\omega$. These correspond to a phonon in the liquid with wave vector q_1 or a roton with wave vector q_2 or q_3.

This problem was analyzed incorrectly by EF because they treated the three solutions as giving three independent, degenerate N-body wave functions Ψ_1, Ψ_2, and Ψ_3. In fact the Ψ_α are merely three different trial functions in a variational theory. They may be combined to form an improved trial function. When optimized, the combined function gives a lower energy and it also determines the reflection coefficient above the roton threshold and the relative probability for conversion to a phonon or one of the two roton states.

The improved function is

$$\Psi=\sum_{\alpha=1}^{3} c_\alpha\Psi_\alpha=\sum_{i=1}^{N}\sum_{\alpha=1}^{3} c_\alpha(\phi_i^\alpha/\sqrt{\rho_i})\Psi_0 , \tag{A1}$$

where $\Psi_0(\mathbf{r}_1,\ldots,\mathbf{r}_N)$ is the ground state of the liquid containing N atoms and with a surface. The functions $\phi_i^\alpha\equiv\phi^\alpha(\mathbf{r}_i)$ are the three solutions to the single-particle integro-differential equation in EF. The c_α are chosen to minimize the expectation value of the energy $\langle E\rangle=\langle\Psi\mid H\mid\Psi\rangle/\langle\Psi\mid\Psi\rangle$. Using the Lagrange multiplier ε and minimizing $\langle\Psi\mid H\mid\Psi\rangle-\varepsilon\langle\Psi\mid\Psi\rangle$ gives the three equations

$$\sum_{\alpha=1}^{3} c_\alpha m_{\alpha\beta}=0,\quad(\beta=1,2,3) , \tag{A2}$$

where

$$m_{\alpha\beta}=h_{\alpha\beta}-\varepsilon g_{\alpha\beta} , \tag{A3}$$

and

$$h_{\alpha\beta}=\langle\Psi_\alpha\mid H\mid\Psi_\beta\rangle,\quad g_{\alpha\beta}=\langle\Psi_\alpha\mid\Psi_\beta\rangle .$$

The matrix elements $h_{\alpha\beta}$, $g_{\alpha\beta}$ have contributions from the "liquid" and the "vacuum" proportional to the volume of these regions. Because of the factors $1/\sqrt{\rho_i}$ in Ψ, the liquid and vacuum contributions are comparable in magnitude. There is also a surface contribution which is negligible for a large volume-to-area ratio.

The volume contributions to $h_{\alpha\beta}$ and $g_{\alpha\beta}$ may be calculated from the asymptotic forms for ϕ^α:

$$\begin{aligned}&\phi_\alpha=A_\alpha e^{ik_x x}(e^{-ik_z z}+R_\alpha e^{ik_z z}),\quad z\to\infty\\&\phi_\alpha=e^{ik_x x}e^{-iq_{\alpha z}z},\quad z\to-\infty\end{aligned} \tag{A4}$$

where k_x is the wave vector of the atom parallel to the surface, and R_α is the complex reflection probability amplitude in the state Ψ_α. The complex quantities A_α are determined by the integro-differential equation. As shown below, they are related to the R_α. The three q_α, the phonon and roton wave vectors, are different from each other, so the liquid region only contributes to the diagonal matrix elements $m_{\alpha\alpha}=h_{\alpha\alpha}-\varepsilon g_{\alpha\alpha}$.

Now consider the contributions from the vacuum region. These are proportional to

$$m^v_{\alpha\beta}=DA^*_\alpha A_\beta(1+R^*_\alpha R_\beta) , \tag{A5}$$

where the quantity D is independent of α and β. As explained in EF, each Ψ_α represents a state in which the particle current of atoms in the vacuum is equal to the particle current of phonons (or rotons) in the liquid. Consequently $\mid A_\alpha\mid$ and $\mid R_\alpha\mid$ are related:

$$\mid A_\alpha\mid^2=\frac{q_{\alpha z}q_\alpha}{k_z\omega}\frac{d\omega}{dq_\alpha}\Big/(1-\mid R_\alpha\mid^2) . \tag{A6}$$

If the phonon channel ($\alpha=1$) is totally reflected, then $\mid R_1\mid=1$ and $\mid A_1\mid$ is infinite.

The reflection amplitude in the improved state Ψ is

$$R=\sum_\alpha c_\alpha A_\alpha R_\alpha\Big/\sum_\alpha c_\alpha A_\alpha . \tag{A7}$$

The coefficients $(c_\alpha A_\alpha)$ are given by a modification of (A2):

$$\sum_\alpha(c_\alpha A_\alpha)(m_{\alpha\beta}/A_\alpha)=0 . \tag{A8}$$

When $\mid R_1\mid=1$, all the elements of the matrix $(m_{\alpha\beta}/A_\alpha)$ remain finite except for m_{11}/A_1. From (A5), m_{11}/A_1 has magnitude

$$\mid m^v_{11}/A_1\mid=D\mid A_1\mid(1+\mid R_1\mid^2) , \tag{A9}$$

which is infinite because $\mid A_1\mid$ is infinite. Consequently, from (A8), c_1A_1 is zero and, from (A7), the reflection amplitude is solely determined by the roton amplitudes R_2 and R_3. If it were not for the excitation of ripplons, this would give a very large decrease in the reflectivity at the roton threshold if the phonon channel were totally reflected.

Even when the roton wave vectors are close to the value at the roton minimum q_0, the contributions to the matrix elements from each roton channel are unequal. (Remember that the two kinds of rotons have different momenta in the z direction, so that Ψ_2 and Ψ_3 are different even at the roton minimum.) This implies that the "anomalous" kind of roton, whose velocity $d\omega/d\mathbf{q}$ is opposite to its momentum $\hbar\mathbf{q}$, is produced at a different rate from that of the ordinary kind, where velocity and momentum are parallel. The production of anomalous rotons by atoms[16] or the reverse process, the evaporation of atoms by anomalous rotons,[19,20] has not been observed experimentally. It is plausible that the matrix elements for these processes are smaller than for those involving ordinary rotons, since much more momentum must be transferred to the center of mass of the liquid.

[1]D. O. Edwards, P. P. Fatouros, G. G. Ihas, P. Mrozinski, S. Y. Shen, F. M. Gasparini, and C. P. Tam, Phys. Rev. Lett. **34**, 1153 (1975).
[2]V. U. Nayak, D. O. Edwards, and N. Masuhara, Phys. Rev. Lett. **50**, 990 (1983).
[3]D. O. Edwards, P. P. Fatouros, and G. G. Ihas, Phys. Lett. **59A**, 131 (1976).
[4]For convenience we take k_z to be positive. Since the z-axis points out from the liquid, k_z can be considered as the perpendicular momentum after reflection.
[5]D. O. Edwards and P. P. Fatouros, Phys. Rev. B **17**, 2147 (1978).
[6]I. B. Mantz and D. O. Edwards, Phys. Rev. B **20**, 4518 (1979).
[7]D. S. Sherrill and D. O. Edwards, Phys. Rev. B **31**, 1338 (1985); J. M. Valles, R. M. Heinrichs, and R. B. Hallock, Phys. Rev. Lett. **56**, 1704 (1986).
[8]I. B. Mantz, Ph.D. dissertation, Ohio State University (1980) (unpublished). The calculated surface tension is $\sigma=0.41$ erg/cm^2, compared to the experimental value $\sigma=0.354$ erg/cm^2 from Ref. 15.
[9]V. R. Pandharipande, S. C. Pieper, and R. B. Wiringa, Phys. Rev. B **34**, 4571 (1986).
[10]P. M. Echenique and J. B. Pendry, Phys. Rev. Lett. **37**, 561 (1976); J. Phys. C **9**, 3183 (1976).
[11]R. P. Feynman, Phys. Rev. **94**, 262 (1954).
[12]T. Usagawa, Phys. Lett. **73A**, 339 (1979).
[13]F. O. Goodman and N. Garcia, Phys. Rev. B **33**, 4560 (1986).
[14]P. M. Echenique and J. B. Pendry (private communication).
[15]M. Iino, M. Suzuki, and A. J. Ikushima, J. Low Temp. Phys. **61**, 155 (1985).
[16]D. O. Edwards, G. G. Ihas, and C. P. Tam, Phys. Rev. B **16**, 3122 (1977).
[17]D. O. Edwards, J. R. Eckardt, and F. M. Gasparini, Phys. Rev. A **9**, 2070 (1974).
[18]M. J. Baird, F. R. Hope, and A. F. G. Wyatt, Nature **304**, 325 (1983).
[19]F. R. Hope, M. J. Baird, and A. F. G. Wyatt, Phys. Rev. Lett. **52**, 1528 (1984).
[20]S. Balibar, J. Buechner, C. Castaing, C. Laroche, and A. Libchaber, Phys. Rev. B **18**, 3096 (1977).
[21]C. Caroli, B. Roulet, and D. Saint-James, Phys. Rev. B **13**, 3875 (1976); **13**, 3884 (1976).